Intermetallics 84 (2017) 130–135

Contents lists available at ScienceDirect

Intermetallics

journal homepage: www.elsevier.com/locate/intermet

Comparative study of R-phase martensitic transformations in TiNi-based shape memory alloys induced by point defects and precipitates

P.C. Chang [a], M.L. Ko [a], B. Ramachandran [a], Y.K. Kuo [a, *], C. Chien [b], S.K. Wu [b]

[a] Department of Physics, National Dong Hwa University, Hualien, 97401, Taiwan
[b] Department of Materials Science and Engineering, National Taiwan University, Taipei, 10617, Taiwan

ARTICLE INFO

Article history:
Received 3 December 2016
Received in revised form
12 January 2017
Accepted 13 January 2017

Keywords:
Shape memory alloys
Martensitic transformation
Electrical properties
Thermal properties
Point defect

ABSTRACT

We studied the influence of point defects (Fe) and precipitates (Ti_3Ni_4) on the characteristics of R-phase martensitic transformation by comparing the transport and thermal properties of as-quenched $Ti_{50}Ni_{46}Fe_4$ and annealed $Ti_{48.7}Ni_{51.3}$ shape memory alloys. Both alloys undergo a weak first-order R-phase transformation with a small thermal hysteresis (less than 7 K) and non-zero transformation strain, suggesting the introduction of point defects and precipitates lead to a stable R-phase in these alloys due to the defects induced local lattice deformations. Furthermore, our study revealed that the transition temperature, transformation width, and transformation strain of the investigated R-phase TiNi-based alloys are strongly affected by the induced defects. As a result, the annealed $Ti_{48.7}Ni_{51.3}$ has a higher transition temperature than that of $Ti_{50}Ni_{46}Fe_4$, as expected.

1. Introduction

TiNi-based shape memory alloys (SMAs) are highly attractive and practical materials because they possess both functional and smart properties [1–3]. Some of the unique properties of these alloys are superior shape memory effect (both one-way and two-way), pseudoelasticity, low elastic anisotropy, high corrosion and abrasion resistance, etc. [2]. Upon cooling or applied stress, near-equiatomic TiNi SMAs transform into a monoclinic structure (martensite B19′) with or without an intermediate R-phase (trigonal, formerly acknowledged as rhombohedral) from a cubic B2 austenite. Importantly, the R-phase transformation has thermoelastic characteristics like the martensitic transformation B2↔B19′ [2,4]. Therefore, TiNi-based alloys with R-phase transformation have the functional properties such as shape memory effect and superelasticity.

The transformation strain associated with the B2↔R is very small (~1%) as compared to that of the B2↔B19 and B2↔B19′ (~8–10%) [2,5]. As a result, the R-phase TiNi alloys have many other salient characteristics such as small thermal hysteresis [2,6], fast response to temperature change [2,7,8], high stability under mechanical/thermal cycling [8,9], and good fatigue resistance [7,10]. Hence, the R-phase TiNi alloys have potential for commercial applications, especially in engineering and medical industries.

It has been reported that the R-phase can be induced via different methods into TiNi-based SMAs, namely i) the introduction of plastic deformation into TiNi-based SMAs to produce the nanocrystals embedded in a solid amorphous matrix [11,12], ii) cold rolling of TiNi-based SMAs to create dislocations [2,13,14], iii) aging or thermal cycling of Ni-rich TiNi to produce rhombohedral Ti_3Ni_4 precipitates [2,14–17], and iv) alloying of TiNi with Fe and Co, etc., to induce point defects [2,18–21]. Importantly, a small composition change could lead to a stable R-phase in TiNi due to the Fermi surface nesting, i.e. the electronic band structure of TiNi can be significantly altered by inducing defects or disorders [22,23]. Accordingly, the hardening of soft-phonon in the B2 phase occurs which accompanies the R-phase martensitic transformation.

The transition temperature of TiNi-based SMAs can also be tuned by changing the composition. However, the shape memory effect and related characteristics in TiNi vary in a complex way with the alloy's composition, i.e. both the structure and defect chemistry play major roles [20]. Recently, Ji et al. suggested that the aforementioned methods (ii-iv) for achieving a stable R-phase in TiNi have the same origin [24]: the competition between a) the thermodynamic driving force for the formation of R-phase and b) the kinetic slowdown of the R-phase formation due to the frustration of

* Corresponding author.
E-mail address: ykkuo@mail.ndhu.edu.tw (Y.K. Kuo).

http://dx.doi.org/10.1016/j.intermet.2017.01.008
0966-9795/

induced defects [11–21]. Importantly, the strength of these two factors could lead to weak local barriers in the TiNi lattice via the induced stress field, which stabilizes the R-phase [24].

In the case of Fe-substituted TiNi ($Ti_{50}Ni_{50-x}Fe_x$), a one-stage B2→R transition is observed for x = 3–5 at.% [18,25]. On the other hand, the introduction of nanosize precipitates (Ti_3Ni_4) into Ni-rich TiNi SMAs with Ni ≥ 51.3 at% also leads to a single R-phase transition via low-temperature aging treatment with optimal annealing times of 24–100 h [17]. With short annealing time, such as less than 10 h, the strain glass characteristics (short-range strain order) are predominately seen in the low-temperature annealed $Ti_{48.7}Ni_{51.3}$ SMAs [17,26]. Moreover, the B2↔R transition temperature of annealed Ni-rich TiNi is higher than that of Fe-substituted TiNi [15-168]. This is essentially due to the larger size of Ti_3Ni_4 precipitates as compared to the point defects [15].

In this work, the characteristics of R-phase transition in two systems, namely Fe-substituted TiNi ($Ti_{50}Ni_{46}Fe_4$) SMA and annealed Ni-rich TiNi ($Ti_{48.7}Ni_{51.3}$) SMAs at different temperatures, are compared. The effects of point defects (Fe) in as-quenched $Ti_{50}Ni_{46}Fe_4$ and rhombohedral precipitates (Ti_3Ni_4) in annealed $Ti_{48.7}Ni_{51.3}$ on the R-phase transition were investigated by transport and thermal measurements. Both alloys display a weak first-order martensitic transition with non-zero transformation strain. In particular, the induced precipitates in the annealed $Ti_{48.7}Ni_{51.3}$ SMA lead to a stable R-phase transformation near room temperature, which makes it a suitable alloy for practical applications.

2. Experiments

Both $Ti_{50}Ni_{46}Fe_4$ and $Ti_{48.7}Ni_{51.3}$ alloys were prepared using a vacuum arc remelter, as reported in details in Refs. [26–29]. First, the melted ingots were heated at 1173 K for more than 1 h and then hot-rolled into plates of ≈2 mm thickness using a rolling machine. Thereafter, the rolled plates were heated at 1173 K for 1 h and then cooled to room temperature (RT) by water quenching. The quenched $Ti_{48.7}Ni_{51.3}$ samples were subjected to low-temperature annealing (aging) at three different temperatures (T_A = 523, 573, and 623 K) for 24 h to induce precipitation. It is well-known that the precipitation of $TiNi_3$, Ti_2Ni_3, and Ti_3Ni_4 compounds can occur in Ni-rich TiNi during annealing [1]. However, $TiNi_3$ and Ti_2Ni_3 do not precipitate at low temperatures (<650 K). Hence, Ti_3Ni_4 is the only possible compound that can form as precipitates in the annealed $Ti_{48.7}Ni_{51.3}$ samples in the present study. Finally, the surface oxide layer of all samples was removed via etching using an HF: HNO_3: H_2O solution (1: 5: 20 in volume).

For transport and thermal measurements, the samples were cut into a rectangular parallelepiped shape with a dimension of 5.0 × 1.5 × 1.5 mm^3 by a low speed diamond saw. The temperature-dependent electrical resistivity of the samples was measured in both cooling and warming cycles using a standard four-probe technique. The Seebeck coefficient and thermal conductivity were measured simultaneously using a direct heat pulse technique during a warming process. The specific heat was measured using a high-resolution ac calorimeter with chopped light as a heat source. Further details about these techniques can be seen elsewhere [27,28].

3. Results

3.1. Electrical resistivity

Fig. 1a displays the electrical resistivity $\rho(T)$ of as-quenched $Ti_{50}Ni_{46}Fe_4$ in cooling and warming cycles. Upon cooling, the resistivity decreases quasi-linearly with temperature until T_S of ~246 K, which is a typical feature of the metallic austenite B2 phase

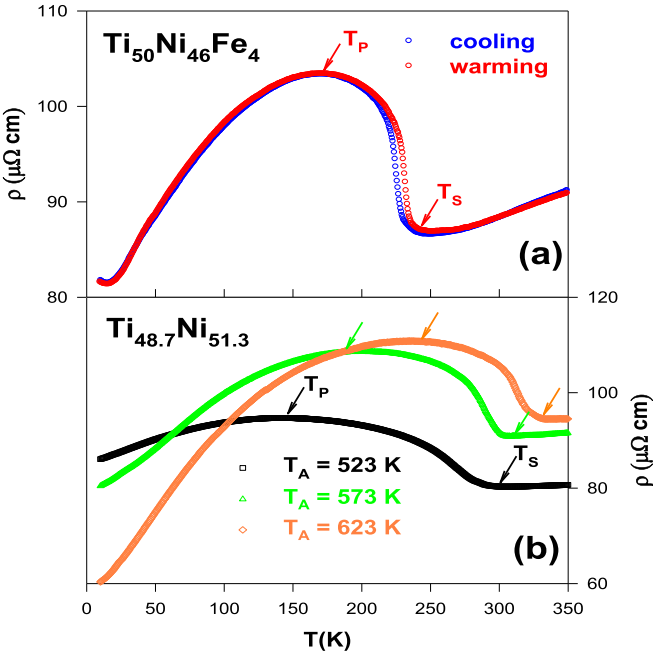

Fig. 1. Temperature-dependent electrical resistivity of a) as-quenched $Ti_{50}Ni_{46}Fe_4$ in cooling and warming cycles and b) the quenched and annealed $Ti_{48.7}Ni_{51.3}$ samples during warming cycle. The annealing temperatures T_A are 523 K, 573 K and 623 K, and the annealing time is 24 h.

above T_S for $Ti_{50}Ni_{46}Fe_4$ [2,24]. With further decreasing temperature, ρ rises quickly below T_S followed by a broad maximum near T_P ~170 K (marked by an arrow in Fig. 1a). Here, T_S is defined as the temperature at which the first derivative of the resistivity changes sign. Importantly, $Ti_{50}Ni_{46}Fe_4$ has a negative temperature coefficient in the range of 246–170 K, which indicates the occurrence of a martensitic transformation B2→R [24,29]. Below T_P, the resistivity decreases gradually with temperature, which indicates the metallic nature of the sample. The warming cycle $\rho(T)$ data of as-quenched $Ti_{50}Ni_{46}Fe_4$ also shows a similar behavior with a transformation R→B2.

Thermal hysteresis of about 7 K is observed for as-quenched $Ti_{50}Ni_{46}Fe_4$ between the cooling and warming cycles, which is much less pronounced than that of the B2↔B19′ transformation exhibited in $Ti_{50}Ni_{50}$ SMA (~35 K) [28]. Nevertheless, the observed transformation has a broader transition width ΔT (= T_S-T_P) of about ~75 K. This could be due to the substituent (Fe) induced variation in the martensitic transformation characteristics, as Fe atoms at different Ni sites of TiNi have a different local environment [30]. Thus, the transition becomes a weak first-order or second-order-like transition. However, there is no feature related to the R→B19′ transition that is expected below 125 K for this sample [29]. This suggests that the transformation terminates at the intermediate R-phase due to the suppression of final transformation R→B19′ [17,18]. In other words, the induced point defects (Fe) completely suppress the B19′ martensite, which has a relatively larger transformation strain [2]. In contrast, the defects hardly affect the stability of R-phase as it associated with the smaller transformation strain. Hence, a one-stage B2→R transition occurs in $Ti_{50}Ni_{46}Fe_4$.

Fig. 1b shows the $\rho(T)$ curves of the quenched and low-temperature annealed $Ti_{48.7}Ni_{51.3}$ samples during the warming cycle. All annealed samples exhibit a one-stage R-phase transition near RT, similar to that of as-quenched $Ti_{50}Ni_{46}Fe_4$ (Fig. 1a). This is presumably due to the formation of a sufficient amount of Ti_3Ni_4